



HAL
open science

Olive Mill Wastewater Valorization in Multifunctional Biopolymer Composites for Antibacterial Packaging Application

Laura Sisti, Grazia Totaro, Nicole Bozzi Cionci, Diana Di Gioia, Annamaria Celli, Vincent Verney, Fabrice Leroux

► **To cite this version:**

Laura Sisti, Grazia Totaro, Nicole Bozzi Cionci, Diana Di Gioia, Annamaria Celli, et al.. Olive Mill Wastewater Valorization in Multifunctional Biopolymer Composites for Antibacterial Packaging Application. *International Journal of Molecular Sciences*, 2019, 20 (10), pp.2376. 10.3390/ijms20102376 . hal-02277260

HAL Id: hal-02277260

<https://hal.science/hal-02277260>

Submitted on 20 Nov 2020

HAL is a multi-disciplinary open access archive for the deposit and dissemination of scientific research documents, whether they are published or not. The documents may come from teaching and research institutions in France or abroad, or from public or private research centers.

L'archive ouverte pluridisciplinaire **HAL**, est destinée au dépôt et à la diffusion de documents scientifiques de niveau recherche, publiés ou non, émanant des établissements d'enseignement et de recherche français ou étrangers, des laboratoires publics ou privés.

Olive Mill wastewater valorization in multifunctional biopolymer composites for antibacterial packaging application

Laura Sisti¹, Grazia Totaro^{1*}, Nicole Bozzi Cionci², Diana Di Gioia², Annamaria Celli¹, Vincent Verney³, and Fabrice Leroux³

¹ Dipartimento di Ingegneria Civile, Chimica, Ambientale e dei Materiali, Università di Bologna, Via Terracini 28, 40131 Bologna, Italy;

² Department of Agricultural and Food Sciences, Università di Bologna, viale Fanin 42, 40127 Bologna, Italy;

³ Institut de Chimie de Clermont Ferrand (ICCF) - UMR 6296 Clermont-Auvergne Université, CNRS, 24 Avenue Blaise Pascal, 63177 AUBIERE (cedex), France;

* Correspondence: grazia.totaro@unibo.it; Tel.: +39 (0)51 2090425

Received: date; Accepted: date; Published: date

Abstract: Olive Mill wastewater (OMW) is the aqueous waste deriving from the production of virgin olive oil. OMW typically contains a wide range of phenol-type molecules, which are natural antioxidants and/or antibacterials. In order to exploit the bioactive molecules and simultaneously decrease the environmental impact of such food waste stream, OMW has been intercalated into the host structure of ZnAl layered double hydroxide (LDH) and employed as integrative filler for the preparation of poly(butylene succinate) (PBS) composites by *in situ* polymerization. From the view point of the polymer continuous phase as well as from the side of the hybrid filler, a focus is performed in terms of molecular and morphological characteristics by gel permeation chromatography (GPC) and X-ray diffraction (XRD); thermal and mechanical properties evaluated by thermogravimetric (TGA), calorimetric (DSC) and dynamic thermo-mechanical analysis (DMTA). Antibacterial properties have been assessed against a Gram-positive and a Gram-negative bacterium, *Staphylococcus aureus* and *Escherichia coli*, respectively, as representatives of potential agents of foodborne illnesses.

Keywords: multifunctional hybrid systems; olive mill wastewater; antibacterial properties; layered double hydroxides; bionanocomposites.

1. Introduction

High-added value compounds, such as pectin and polyphenols, can be recovered from agro-wastes and reused as food ingredients, cosmetics or even in pharmaceutical preparation [1, 2]. Many researches are today devoted to the valorization of agro-food by-products, in order to address sustainable and environmental requirements [3-5]. However, the recovery of target components from waste implies the use of down-stream and purification processes which are time consuming and costly as well as not environmental friendly due to the use of huge amount of water. An alternative approach consists here in exploiting agro-wastes without any pre-treatment, with the aim of preparing multifunctional materials, whose development indeed is now of great interest for the industry, always looking for high performance products obtainable through simple and low-cost processes. In the field of packaging, for example, where preserving the quality and increasing the safety of the products is of crucial importance, the antibacterial, antioxidant and/or anti-UV properties are strongly required. At the same time, in the packaging sector, biopolymers (from natural sources and/or biodegradable) are emerging on the market, because of a growing global pressure, deriving from the extensively publicized effects of climate change, price increase of fossil materials, as well as depletion of global fossil resources [6]. However, biobased materials do not achieve technical performances comparable to their fossil counterparts.

A straightforward strategy that allows the obtainment of high performance and multifunctional materials involves the use of organo-modified layered double hydroxides (LDHs) dispersed in polymeric matrices. LDHs are a class of anionic clays, consisting of stacked brucite-type $[Mg(OH)_2]$ octahedral layers with water molecules and exchangeable anions in the interlayer region, offering a large variety of hetero-structured materials [7]. Thanks to their great versatility, as well as simple preparation, the LDH host structures are often considered as a toolbox and their applications are strongly diversified, ranging from catalysis to biomedical, cosmetics, functional additives and/or stabilizers in polymer formulations, sorbents and scavengers for pollutants [8, 9].

Our research group is profoundly concerned to target green fillers in association with bio-based and biodegradable polymer. Our previous researches have demonstrated that the use of organo-modified LDHs may provoke a significant chain extension effect on polymer matrices with consequent improvement of their processability [10-14]. Moreover, suitable properties, such as antioxidant/antibacterial/anti-UV, due to the tethered / intercalated anions into the LDH, can be exploited, leading to multifunctional fillers. LDH acts as inorganic cargo hosting bioactive molecules and it protects them from thermal degradation, thus enhancing their thermal stability as well as allowing the preservation of their bioactivity, well-maintained under such protective layer against injection / extrusion during polymer composites processing [15, 16]. Therefore, multifunctional composite materials with antioxidant/antibacterial/anti-UV properties can be achieved.

More in detail, in a previous work [17], olive mill wastewater (OMW), without any pre-treatment, was successfully intercalated into a Zn_2Al -LDH with the aim of enhancing the durability of polypropylene (PP) and poly(butylene succinate) (PBS) melt blended composites. In the current study, the antibacterial and the thermomechanical properties of similar systems have been further investigated. Therefore, the materials prepared can be suitable for antibacterial/antioxidant coating and packaging, as well as medical devices and household products.

OMW is a high organic load and recalcitrant waste stream of great environmental concern and its management is a very important issue in Mediterranean countries because of the huge amount of olives: more than 2.4 million tons/year, whose 90% is meant for olive oil production, thus up to 30 million m^3 per year of OMW is generated [17, 18]. The composition of OMW consists in 80–90% water, 4–16% organic compounds (such as tyrosol, hydroxytyrosol, p-coumaric acid, ferulic acid, syringic acid, protocatechuic acid, vanillic acid tannins, anthocyanins, etc.) and 0.4–2.5% mineral salts (K, Ca, Na). Due to their low partition coefficients, the olive phenols are more soluble in water than in oil phase. Thus, polyphenols are found in OMW at concentrations ranging from 0.03–11.5 g/L according to the processing system used for olive oil production [1].

Among biobased polyesters, PBS is of particular interest. It is a biodegradable semi-crystalline polymer, whose both pristine monomers (1,4-butanediol and succinic acid) can be obtained from sugar fermentation. PBS is emerging in agriculture, consumer goods and especially in flexible packaging market [6]. Due to its thermal and mechanical characteristics, PBS ranks similar to PP for its strength (tensile strength 34 MPa for PBS and 33 MPa for PP) and between low-density (LDPE) and high-density polyethylene (HDPE) for its stiffness (flexural modulus 656 MPa for PBS, 176 MPa for LDPE, 1070 MPa for HDPE) [19, 20].

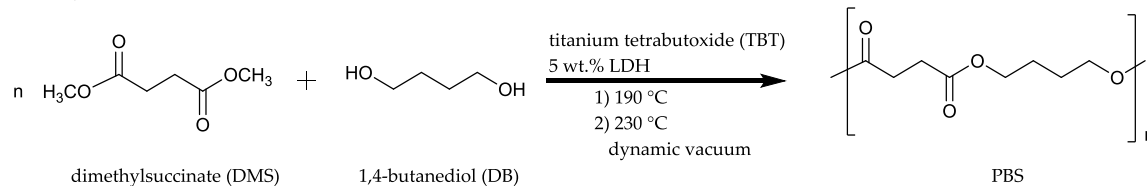
In details, OMW was here used as intercalating agent in layered Zn_2Al -LDH, i.e. between its organo-modified platelets; some phenol model molecules, as typical chemical structures of the main components present in OMW (namely vanillic acid VA, ferulic acid FA, protocatechuic acid PA) were also employed, for comparison. Mixed systems were also prepared, by simultaneous coprecipitation of two or three biomolecules, to simulate a medium containing more than one bioactive compound, as in OMW. The organo-modified LDHs (5 wt. %) were employed for the preparation of PBS composites through *in situ* polymerization. Both the organo-modified LDHs and the obtained composite samples were tested for their anti-microbial action against *Escherichia coli* and *Staphylococcus aureus*. Thermal and thermo-mechanical properties were investigated by TGA, DSC and DMTA.

2. Results and Discussion

A full characterization of the prepared LDH samples, as well as the total organic compound (TOC) of the biowaste (4.51 ± 0.65 g GA eq/L, GA = gallic acid), were reported elsewhere [17]. Briefly, HPLC analysis revealed the presence of protocatechuic acid, vanillic acid, trans-cinnamic acid, gallic acid and chlorogenic acid in OMW. FT-IR and X-ray analyses of the LDHs containing vanillic acid (Zn_2Al/VA), ferulic acid (Zn_2Al/FA), protocatechuic acid (Zn_2Al/PA) demonstrated the intercalation of the anions between the lamellae. Mixed systems were also prepared, by simultaneous coprecipitation of FA and PA ($Zn_2Al/FA-PA$), or VA, FA and PA ($Zn_2Al/VA-FA-PA$), to simulate a medium containing more than one bioactive molecule, as in OMW. Concerning such systems and the sample intercalated with OMW (Zn_2Al/OMW), a selective interaction with some molecules was evident from FT-IR, but from X-ray diffraction analysis, it was concluded that the coprecipitation of LDH in presence of OMW was not 100% efficient in yielding LDH structure, giving rise to another inorganic material ($\gamma-AlOOH$) unable to trap organic guest. This was confirmed by a lower organic weight loss % from TGA in Zn_2Al/OMW . Therefore, in such sample (Zn_2Al/OMW) the two structures (LDH and $\gamma-AlOOH$) are concomitantly present. The thermal protecting role of the LDH towards the anions was clear from TGA analysis because the thermal stability was enhanced after intercalation. This is a key point in this strategy because it allows the preservation of the bioactivity, well-maintained under such protective layer during polymer composite processing.

In the current study, 5 wt. % of the organic/inorganic (O/I) hybrid fillers was employed to prepare PBS bionanocomposites by *in situ* polymerization, which is an effective method to reach a good state of dispersion for the LDH filler. Such loading was reported to be appropriate, in similar systems, to assure the persistence of bioactivity [16, 17, 21]. Scheme 1 shows the monomers employed and the conditions of the *in situ* polymerization process. The bionanocomposites have been labelled PBS: Zn_2Al/X , according to the LDH employed.

The molecular weights of all composites, obtained by GPC analysis, resulted to be high, into the range $50 \cdot 10^3 < M_w < 90 \cdot 10^3$ g/mol with polydispersity values coherent to common polyesters ($M_w/M_n \approx 2$) (Table 1).



Scheme 1. *In situ* polymerization of PBS bionanocomposites.

Table 1. GPC and TGA results of PBS, PBS:FA/PA and PBS: Zn_2Al/X composites.

Sample	M_w ($\times 10^{-3}$ g mol ⁻¹) ^{a)}	M_w/M_n ^{a)}	T_{onset} (°C) ^{b)}	T^{10}_D (°C) ^{b)}	T_{max} (°C) ^{b)}
PBS	69	2.4	380	363	406
PBS: Zn_2Al/VA	91	2.4	353	344	393
PBS: Zn_2Al/FA	47	2.2	357	340	393
PBS: Zn_2Al/PA	49	2.3	355	347	389
PBS: $Zn_2Al/FA-PA$	61	2.3	355	338	395
PBS: $Zn_2Al/VA-FA-PA$	68	2.5	345	341	387
PBS: Zn_2Al/OMW	61	2.4	355	347	387
PBS:FA/PA	8	2.7	376	360	403

^{a)} Determined by GPC in $CHCl_3$; ^{b)} Determined by TGA under air flow.

PBS:FA/PA, without LDH, with 1 wt. % of FA and 1 wt. % of PA respect to the polymer theoretical yield, was also prepared in order to better understand the beneficial role of LDH. Of course, during the polymerization, FA and PA compete with DMS in the condensation reaction with BD, therefore a copolymer is formed. ¹H NMR shows that only 0.32 mol % of both FA and PA has

copolymerized. The results of GPC analysis indicate that oligomers were formed ($M_w = 8 \cdot 10^3$ g/mol) because FA and PA possess only one reactive functional group, therefore they act as chain stopper during the macromolecular growth.

The degree of dispersion of the organo-modified LDHs in PBS matrix was evaluated by XRD analysis. In Figure 1, since the same results were obtained for all the samples, only some representative composite XRD patterns were reported, showing the diffraction lines characteristic of PBS and the absence of the diffraction peaks of the associated filler. This can be explained by a low crystallinity of the filler or by a potential exfoliation occurring during thermal processing. All the characteristic peaks ascribable to the crystalline structure of PBS (020) (021) (110) (111) can be found in 2θ range 18-30° and no significant difference can be depicted with PBS free of filler. The copolymer presents narrow diffraction lines, due to PBS crystallinity.

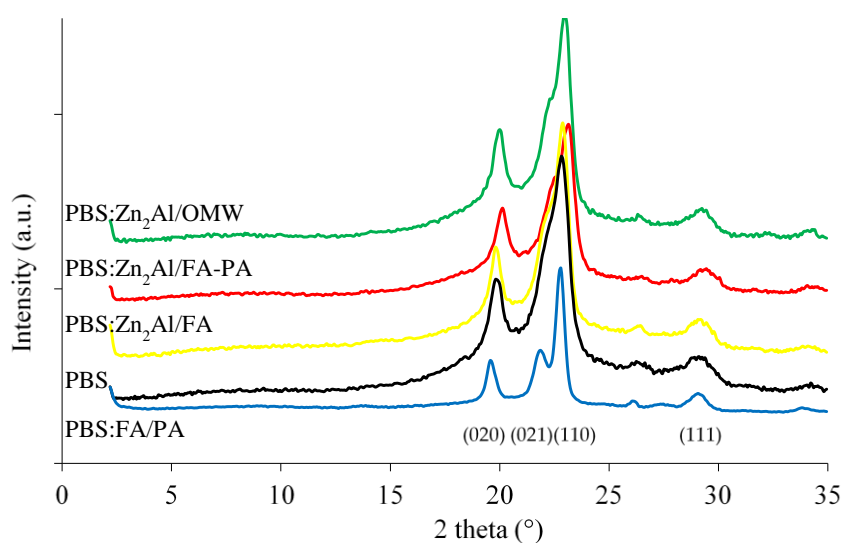


Figure 1. XRD profiles of PBS and some PBS:Zn₂Al/X composites with indexing of the main reflections due to crystalline structure of PBS.

Table 1-2 enlist all the results from TGA and DSC analyses of the nanocomposites. From figure 2, reporting TGA thermograms of all the samples, a main decomposition process is depicted in the temperature range 360–375 °C. Concerning the nanocomposites, the filler does not exert a thermal stabilization upon the matrix, because of the catalyzing effect of metals, as well as the polyester hydrolysis promoted by the water released during its thermal degradation. In any case, the thermal data reported (T_{onset} , T^{10D} , T_{max}) are consistently higher than the melting temperature of PBS (116 °C): therefore, such expected thermal degradation are overcome during processing. This is consistent with literature [12, 13]. As expected, the copolymer shows initial and maximum degradation temperatures close to PBS.

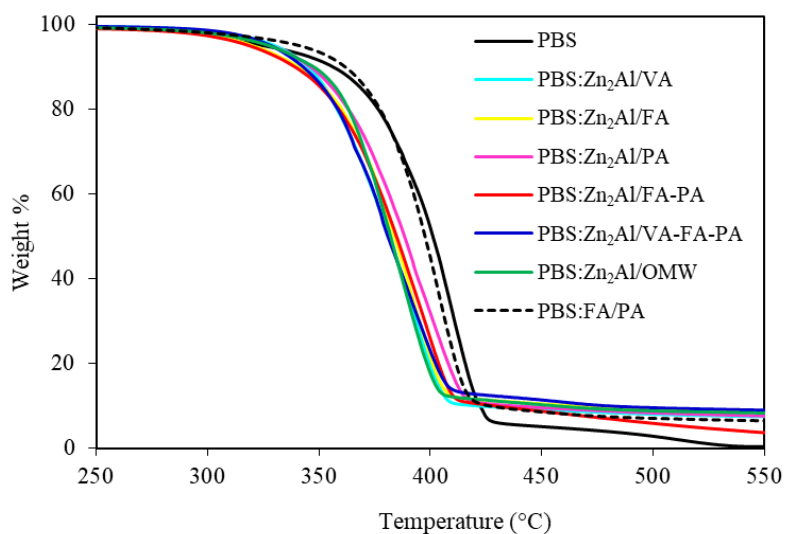


Figure 2. TGA profiles of PBS, PBS:FA/PA and PBS:Zn₂Al/X composites.

From DSC analysis reported in Table 2, it can be noted that T_m values of the nanocomposites slightly decrease respect to 116 °C (melting temperature of PBS). Moreover, the peak shapes are complex and multiple endothermic peaks are present, due to the melting-recrystallization process, generally occurring in polyesters [22]. Concerning the cooling scan, most of composites crystallize at higher temperature respect to PBS, while PBS:Zn₂Al/OMW has lower T_c . However, all the composites present lower ΔH_c respect to PBS, therefore the motion of the polymer chains in the melt are restricted by the platelets and the crystallization process is somehow hindered. Indirectly this behavior confirms a good degree of dispersion of the LDHs in the PBS matrix.

Table 2. Thermo-mechanical results of PBS, PBS:FA/PA and PBS:Zn₂Al/X.

Sample	T_g (°C) ^{a)}	T_g (°C) ^{b)}	T_c (°C) ^{c)}	ΔH_c (J g ⁻¹) ^{c)}	T_m (°C) ^{b)}	ΔH_m (J g ⁻¹) ^{b)}
PBS	-16.3	-33	70	72	116	77
PBS:Zn ₂ Al/VA	-14.4	-35	73	64	113	64
PBS:Zn ₂ Al/FA	-8.9	-36	73	52	113	47
PBS:Zn ₂ Al/PA	-8.9	-34	76	53	115	48
PBS:Zn ₂ Al/FA-PA	-8.9	-36	77	55	114	51
PBS:Zn ₂ Al/VA-FA-PA	-13.4	-36	77	61	114	58
PBS:Zn ₂ Al/OMW	-13.4	-36	66	51	114	57
PBS:FA/PA	/	-30	66	62	110	67

^{a)} Determined by DMTA; ^{b)} Determined by DSC during the 2nd heating scan;

^{c)} Determined by DSC during the cooling scan from the melt at 10 °C min⁻¹.

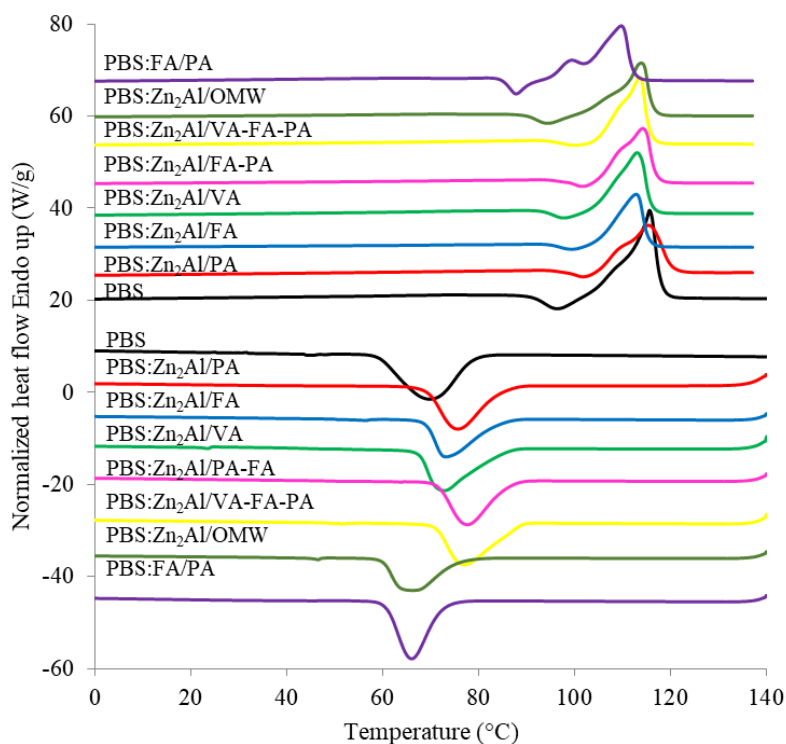


Figure 3. DSC profiles of PBS, PBS:FA/PA and PBS:Zn₂Al/X composites.

In order to evaluate the mechanical properties of the samples prepared, dynamic thermo-mechanical analysis (DMTA), which measures the response of a material to a cyclic deformation as a function of the temperature, has been performed. Figure 4 shows the storage modulus E' and $\tan \delta$, which is the ratio of the loss modulus to storage modulus, as a function of temperature. The nanocomposites, respect to the homopolymer, present superimposable curves, with E' values slightly higher than PBS within all the temperature range, this revealing a reinforcing role of the O/I hybrid filler upon PBS. Additionally, it highlights an efficient interface interaction between the filler and the polymer, as well as a good state of dispersion of LDH platelets. The reinforcement effect of the fillers becomes more important above the glass transition temperature, when materials become soft, due to the restricted movement of the polymer chains [23]. At 20 °C the fillers show a medium E' enhancement of 40%, and the maximum value is related to PBS:Zn₂Al/PA (51%). Respect to DSC analysis, DMTA is a more sensitive technique to evaluate T_g (Table 2): the bionanocomposites show higher T_g values respect to PBS (-16.3 °C), this is due to the restriction of the movements of the macromolecular chains, due to their interaction with the nanosheets of organo-modified LDH fillers.

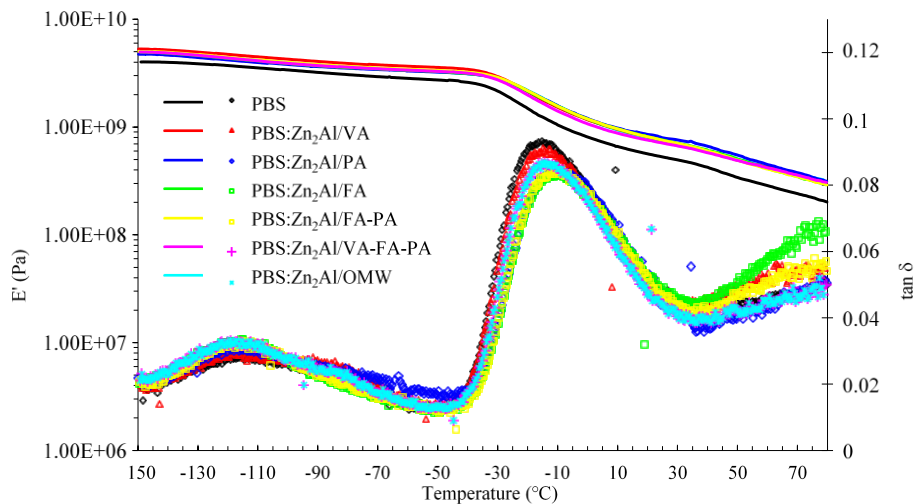


Figure 4. DMTA profiles of PBS and PBS:Zn₂Al/X composites.

The antibacterial properties of both O/I hybrid fillers and nanocomposites have been checked against a Gram-positive bacterium, *S. aureus*, and a Gram-negative one, *E. coli*, which are potential agents of foodborne illnesses causing serious infections [15] and ubiquitous widespread bacteria [24, 25] (Figure 5). The activity is calculated using Equation (1), expressed as percentage of reduction of viable cells in the assayed sample compared to a negative control consisting of a bacterial culture grown in the absence of any material. As a prerequisite for the whole set of experiments, reference materials (PuralMg61 and PBS) were assayed for the antimicrobial evaluation tests, showing no antibacterial effectiveness for PuralMg61 and an antimicrobial activity of 10 and 18% for PBS in the presence of *E. coli* and *S. aureus*, respectively. Hybrid LDHs powders are characterized by a strong antibacterial activity (cell mortality rate = 100%) against *S. aureus* and *E. coli*. Slightly lower values are recorded for Zn₂Al/VA vs *S. aureus* (87%) and Zn₂Al/OMW (94% and 91% vs *E. coli* and *S. aureus*, respectively). In the latter case, the presence in the waste of different phenolic compounds, as well as of other substances, may somehow interfere in the antibacterial activity causing a slightly lower mortality with respect to the use of the pure compounds. However, the percentage of mortality is high (> 90%) also with the OMW-containing samples. These results are in agreement with literature data [26-28] and confirm the strong antimicrobial activity associated to OMW phenolic compounds.

Considering the PBS nanocomposites, the results obtained using 50 mg of each sample on 500 μ L of bacterial cells (10^5 CFU/mL) (Fig. 5a and c) highlight that the antimicrobial activity is maintained in the final products, reaching values of 100% of mortality against *E. coli* and close to 100% against *S. aureus*. In addition, two amounts of PBS:Zn₂Al/OMW (50 mg and 10 mg) were tested using the same suspension of *E. coli* cells (500 μ L), reaching in both cases a cell mortality rate of 100% (not shown in Fig. 5). The slight differences in the antibacterial properties could be due to the different architecture of the outer layers of Gram positive and negative bacteria that may favour the antibacterial action of lipophilic molecules in Gram negative cells. Indeed *E. coli* has an extra lipopolysaccharide membrane outside a thin cell wall layer, while a thick peptidoglycan wall represents the external envelope in Gram positive bacteria [15]. Phenols are reported both to destroy the external Gram negative layers and to pass through this layer, thus exerting their biocidal activity in the cytoplasm [29]. Indeed, they act specifically on the cell membrane and inactivate intracytoplasm enzymes by forming unstable complexes.

On the other hand, as expected, the copolymer PBS:FA/PA does not present any significant antibacterial activity, thus highlighting the role of LDH in protecting the bioactivity of the organic

modifiers during the polymerization process. Indeed the inorganic host thermally protects the intercalated molecules, thus preserving their bioactivity.

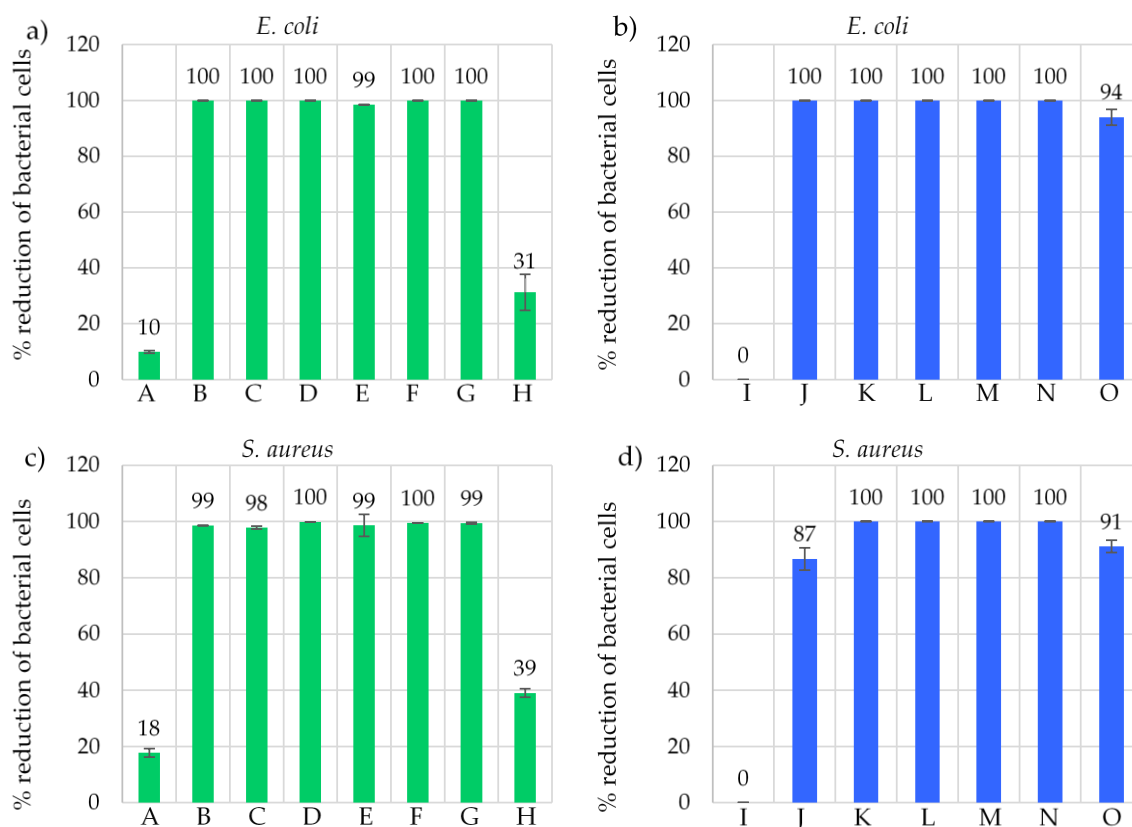


Figure 5. Antibacterial properties of PBS, PBS:FA/PA, bionanocomposites (left side), and LDHs (right side) against *E. coli* (a and b) and *S. aureus* (c and d). A = PBS, B = PBS:Zn₂Al/VA, C = PBS:Zn₂Al/FA, D = PBS:Zn₂Al/PA, E = PBS:Zn₂Al/FA-PA, F = PBS:Zn₂Al/VA-FA-PA, G = PBS:Zn₂Al/OMW, H = PBS:FA/PA, I = PuralMg61, J = Zn₂Al/VA, K = Zn₂Al/FA, L = Zn₂Al/PA, M = Zn₂Al/FA-PA, N = Zn₂Al/VA-FA-PA, O = Zn₂Al/OMW.

To evaluate if such high activity in the case of the hybrid LDH materials can be due to phenolic acids potentially released from the LDH surface into the test medium, release studies of VA (as target bioactive molecule) from Zn₂Al/VA and PBS:Zn₂Al/VA have been carried out (Figure 6). The results show a maximum release of 300 mg/L from Zn₂Al/VA in saline but, most importantly, a negligible release is obtained for the corresponding nanocomposite (maximum 9 mg/L). The released VA cannot be responsible for the inhibitory activity against the target microorganisms, considering that the minimal inhibitory concentration (MIC) of VA is 500 mg/L vs *E. coli* (although a partial inhibition can also be seen at 300 mg/L) and higher than 500 mg/L vs *S. aureus*, i.e. higher amounts with respect to those released from the specimens (Table 3).

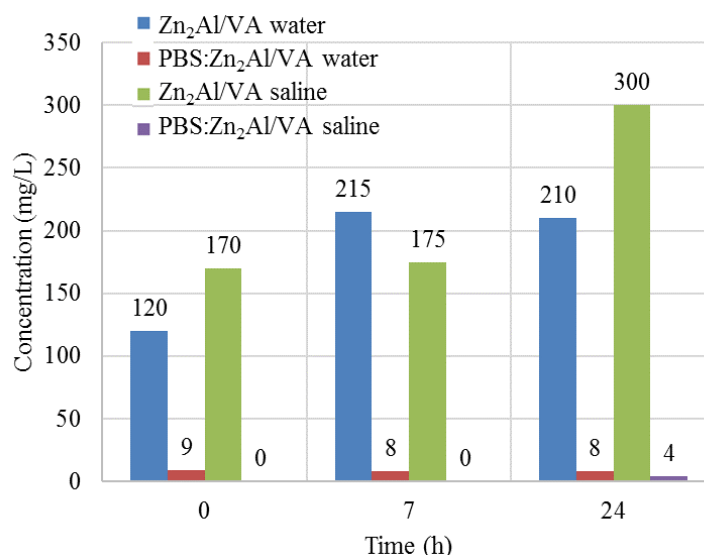


Figure 6. Concentration of vanillic acid evaluated by HPLC analyses in water or saline in which samples have been immersed.

Table 3. Minimal inhibitory concentration (MIC) of vanillic acid (taken as target bioactive molecule) vs *E. coli* and *S. aureus*. Strain growth is reported as turbidity in the McFarland scale. Values represent the difference between the turbidity measured after 24 h of incubation at 37 °C and that detected at the beginning of the incubation.

[Vanillic acid] mg/L	Growth after 24 h of incubation	
	<i>E. coli</i>	<i>S. aureus</i>
500	0.175 ± 0.025	1.385 ± 0.016
300	0.495 ± 0.015	3.235 ± 0.031
150	1.240 ± 0.023	3.585 ± 0.021
75	2.800 ± 0.018	4.24 ± 0.017
0	3.250 ± 0.026	4.935 ± 0.024

The potential of using OMW as antimicrobial agent was confirmed by the data obtained with LDH and PBS nanocomposites containing the waste as it is. These results demonstrated that it is possible to obtain optimal antimicrobial performances also by using OMW without any pre-treatment, potentially leading to a true recycling and valorization of this bio-waste in the development of multifunctional materials.

4. Materials and Methods

4.1. Materials

1,4-butanediol (BD), dimethyl succinate (DMS), sodium hydroxide, aluminum nitrate $\text{Al}(\text{NO}_3)_3 \cdot 9\text{H}_2\text{O}$, zinc nitrate $\text{Zn}(\text{NO}_3)_2 \cdot 6\text{H}_2\text{O}$, vanillic acid (VA), trans-ferulic acid (FA), protocatechuic acid (PA), ethanol and titanium tetrabutoxide (TBT) were purchased from Aldrich Chemical. All the

materials were used as received. Nutrient broth and plate count agar were from Oxoid, Basingstoke, UK. McFarland turbidity standards were from Biolife, Italy. The olive mill wastewater (OMW) was furnished by Sant'Agata d'Oneglia (Imperia, Italia) and concentrated prior to use: from 10 L, 1 L was obtained. Its main chemical features were: Chemical Oxygen Demand (COD) 43.5 ± 1.6 g/L; Total Organic Compound (TOC) 4.51 ± 0.65 g GA eq/L (GA = gallic acid); Total Suspended Solids (TSS) $39,200 \pm 4,808$ mg/L.

4.2. LDHs synthesis

The LDHs have been prepared by coprecipitation following a procedure described elsewhere [17] with OMW, VA, FA, PA. Two co-intercalated LDHs with mixtures of FA+PA, and VA+FA+PA, were also prepared. Briefly, 50 mL of deionized water solution containing 31.2 mmol of $Zn(NO_3)_2 \cdot 6H_2O$ and 15.6 mmol of $Al(NO_3)_3 \cdot 9H_2O$ was added dropwise, during 3h, in a reactor containing 62.4 mmol of the anion in 100 mL of ethanol/deionized water (60/40) under vigorous stirring. In case of OMW, 60 mL have been used. The pH was maintained at $9.5 (\pm 0.1)$ through addition of NaOH solution. The reaction was carried out under nitrogen atmosphere and stirred for 3 h, at room temperature. The solid material was separated and submitted to 3 cycles of deionized washing/ethanol centrifugation. The sample were labeled as Zn_2Al/X , where X is the anion. A full characterization of the LDHs (X-ray diffraction, FT-IR and TGA analysis) is reported elsewhere [17].

4.3. Bionanocomposites preparation

Bionanocomposites with 5 wt. % loading of the organo-modified LDHs were prepared by *in situ* polymerization following a common procedure already reported [30]. As an example, the procedure for preparing PBS: Zn_2Al/VA is described: a round-bottomed, wide-neck glass reactor (250 mL capacity) was loaded with BD (29.6 g, 328 mmol), TBT (0.0585 g, 0.172 mmol) and 2.35 g of Zn_2Al/VA (previously dried overnight at $105^\circ C$), corresponding to 5 wt. % with respect to the polymer theoretical yield. The reactor was closed with a three-necked flat flange lid equipped with a mechanical stirrer and a torque-meter which gave an indication of the viscosity of the reaction melt. The system was then connected to a water-cooled condenser and immersed in a thermostatic salt-bath at $190^\circ C$, under vigorous stirring. After one hour, DMS (40.0 g, 274 mmol) was added and the mixture was kept at $190^\circ C$ until all the methanol distilled off. Then the reactor was connected to a liquid nitrogen-cooled condenser and dynamic vacuum was applied down to 0.5 mbar while the temperature was increased up to $230^\circ C$. When the torque of the melt was around 7-8 mN, a highly viscous, light brown and transparent melt was discharged from the reactor. For comparison, PBS homopolymer was also synthesized, as well as PBS:FA/PA, without LDH with 1 wt. % of FA + 1 wt. % of PA. The molecular structure of PBS was confirmed by 1H NMR. 1H NMR on PBS:FA/PA was conducted on purified sample.

4.4. Antibacterial properties

The antimicrobial properties were assessed by evaluating the survival of bacterial cells exposed to the prepared samples: LDHs intercalated with phenolic acids or OMW, in order to check the antibacterial activity of the active principles, and PBS with 5 wt. % LDHs, to test the efficacy of the final bionanocomposites. The two microorganisms used were *E. coli* ATCC 8739 and *S. aureus* ATCC 6538. Bacteria were grown aerobically in nutrient broth for 16 h at $37^\circ C$. The bacterial culture obtained was centrifuged at 7000 rpm for 10 min, washed in sterile saline (0.9% w/v NaCl) and re-suspended in the same solution in order to obtain $\approx 10^5$ colony forming units (CFU)/mL.

The experiments on both LDHs and composites were performed using 50 mg of powder of each sample, which were put in contact with 500 μL of cells ($\approx 10^5$ CFU/mL in saline) at room temperature (about $23 \pm 1^\circ C$) for 24 h. The same experiment has been preliminarily done with a commercial LDH sample (PuralMg61) and a commercial PBS (i.e. with no added compounds). The composites have been sieved in

order to achieve a homogeneous, fine, particle size. After the incubation, each sample was serially diluted (1:10) and the dilutions were plated on plate count agar. After incubation of the plates at 37 °C for 24 h, the number of colonies corresponding to the number of viable cells was determined, after averaging using triplicates, through a modification of the equation reported by Lala *et al.* [31], as follows:

$$R \% = [(B-A)/B] \times 100 \quad (1)$$

where R % = percentage of reduction of viable cells, A= average number of viable cells obtained after 24 h of contact with sample powders, and B = average number of viable cells after 24 h of incubation of a bacterial cell suspension in the absence of any material. As already mentioned, the commercial powders with no added compounds were also tested for their antimicrobial activity against the same strains.

An additional experiment was carried out only on the bionanocomposite intercalated with OMW (PBS:Zn₂Al/OMW), in order to evaluate the antimicrobial activity with a less concentrated amount of sample: 10 mg of powder were put in contact with 500 µL of *E. coli* cells ($\approx 10^5$ CFU/mL in saline) and incubated as well as the previous experiment.

4.4.1. Minimal Inhibitory Concentration (MIC) of vanillic acid as target compound

Different concentrations of vanillic acid have been tested in order to evaluate the minimal concentration that inhibits the growth of *E. coli* and *S. aureus*. A stock solution of the assayed compound was prepared at a concentration of 10000 mg/L in ethanol 70% (v/v of water). The concentrations tested were: 500 mg/L, 300 mg/L, 150 mg/L and 0 mg/L. Bacterial growth in the presence of vanillic acid at different concentration was monitored by evaluating the turbidity of the culture after 24 h of incubation at 37 °C using a densitometer (DEN1-Biosan) which evaluates turbidity using the MacFarland scale. Commercial McFarland standards (0.0-0.6 McFarland units) were used for calibrating the densitometer. The sample for MIC testing consists of 3 mL of nutrient broth, to which 100 µL of a culture grown overnight (10^8 CFU/mL) and the appropriate volume of vanillic acid from the stock solution were added. The assay was performed in duplicate.

4.4.2. Release study

Release studies of vanillic acid from LDH and nanocomposite to the surrounding environment have been conducted in water and saline on samples containing Zn₂Al/VA and the corresponding composite (50 mg/500 µL), under stirring for 24 h at room temperature. Small aliquots of the supernatants have been analyzed by HPLC at 0, 8, and 24 h of incubation.

4.5. Measurements

¹H NMR spectra were recorded on a Varian Mercury 400 spectrometer (chemical shifts are in part per million downfield from TMS); the solvent used was CDCl₃.

GPC measurements were performed on a HP 1100 Series using a PL gel 5 µm Minimixed-C column with chloroform as eluent and solvent for polymer samples. A Refractive Index detector was used and a calibration plot was constructed with polystyrene standards.

TGA was performed in air atmosphere using a Perkin Elmer TGA7 apparatus (gas flow 30 mL/min) at 10 °C min⁻¹ heating rate from 50 to 900 °C for all the samples. The onset degradation (T_{onset}), 10% mass loss ($T_{10\%}$) and maximum degradation temperatures (T_{max}) were measured.

DSC was carried out, under nitrogen flow, using a Perkin-Elmer DSC6. To erase any previous thermal history, the samples (ca. 10 mg) were first heated at 20 °C min⁻¹ to 140 °C, kept at high temperature for 2 min, cooled down to -60 °C at 10 °C min⁻¹, and heated from -60 °C to 150 °C at 10 °C min⁻¹ (2nd scan). During the cooling scan the crystallization temperature (T_c) and the enthalpy of crystallization (ΔH_c) were measured. During the 2nd heating scan the glass transition temperature (T_g), the melting temperature (T_m) and the corresponding enthalpy (ΔH_m) were measured.

Nanocomposite powder samples have been analysed by XRD in steps of 0.07° over 2θ range of 2.1-35°, at room temperature with Bragg/Brentano diffractometer (XPERT-PRO) with Cu Kα radiation (λ = 0.154 nm, monochromatisation by primary graphite crystal) generated at 40 mA and 40 kV.

Physical and mechanical properties were determined using a Rheometric Scientific DMTA IV Dynamic Mechanic Thermo analysis instrument with a dual cantilever testing geometry. Typical test samples were bars (33 × 8 × 2 mm), obtained by injection moulding at 140 °C using a Minimix Molder. The analysis was carried out from -150 °C to 80 °C (heating rate 3 °C min⁻¹, frequency 3 Hz, strain 0.01%).

5. Conclusions

Layered double hydroxides intercalated by vanillic acid, ferulic acid, protocatechuic acid, olive mill wastewater are dispersed in PBS through *in situ* polymerization. The thermal protecting role of the inorganic host towards the bioactive molecules is here confirmed. DMTA analysis demonstrates that all the fillers endow PBS with a pronounced reinforcing effect. In particular, the nanocomposite with Zn₂Al/PA at 20 °C displays an elastic modulus E' enhanced of more than 50% compared to PBS free of filler.

All the nanocomposites present an impressive antibacterial activity as well as a negligible release of the active agent under the tested conditions. Therefore, these preliminary results highlight the possibility of using OMW as potential agent able to confer antimicrobial activity to nanocomposites, with an important additional value in decreasing the environmental impact towards an offensive food stream. In addition, besides pronounced antimicrobial properties, the phenolic compounds in OMW are proved to exert beneficial effects on human health: PA is reported to be an anticancer agent [32] as well as FA, which has anti-inflammatory, antiviral, immune-protective properties. Both molecules can inhibit cancer by scavenging reactive oxygen species or being involved in cell cycle upon cellular uptake [33]. These points even more support the use of OMW phenolic compounds for applications addressed to human health and care, taking also into account their antioxidant properties, previously demonstrated [17].

Reminiscent of the use of other bio-waste such as lignosulfonated LDH blend with plasticized starch and thermoplastics [34], this could represent a general strategy potentially employable with other bio-wastes.

Author Contributions: Conceptualization, L.S., A.C.; methodology, L.S., A.C., D.D.G., V.V., F.L.; investigation, G.T, N.B.C.; writing—original draft preparation, G.T.; writing—review and editing, all authors.

Funding: This research received no external funding.

Acknowledgments: The authors wish to thank Prof. Lorenzo Bertin for providing OMW and Dr. Andrea Negroni for HPLC analysis.

Conflicts of Interest: The authors declare no conflict of interest.

References

1. El-Abbassi, A.; Saadaoui, N.; Kiai, H.; Raiti, J.; Hafidi, A. Potential applications of olive mill wastewater as biopesticide for crops protection. *Sci. Total Environ.* **2017**, *576*, 10–21.
2. Fritsch, C.; Staebler, A.; Happel, A.; Cubero Márquez, M.A.; Aguiló-Aguayo, I.; Abadias, M.; Gallur, M.; Cigognini, I.M.; Montanari, A.; Jose López, M.; Suárez-Estrella, F.; Brunton, N.; Luengo, E.; Sisti, L.; Ferri, M.; Belotti, G. Processing, Valorization and Application of Bio-Waste Derived Compounds from Potato, Tomato, Olive and Cereals: A Review. *Sustainability* **2017**, *9*, 1492(1-46 pages).
3. Scoma, A.; Pintucci, C.; Bertin, L.; Carlozzi, P.; Fava, F. Increasing the large scale feasibility of a solid phase extraction procedure for the recovery of natural antioxidants from olive mill wastewaters. *Chem. Eng. J.* **2012**, *198-199*, 103-109.

4. Zhu, W.F.; Wang, C.L.; Ye, F.; Sun, H.P.; Ma, C.Y.; Liu, W.Y.; Feng, F.; Abe, M.; Akihisa, T.; Zhang, J. Chemical Constituents of the Seed Cake of *Camellia oleifera* and Their Antioxidant and Antimelanogenic Activities. *Chem. Biodiversity* **2018**, *15*(7),e1800137(1-8 pages).
5. Waldron, K. *Handbook of Waste Management and Co-Product Recovery in Food Processing* 1st Ed.; Woodhead Publishing Limited, Cambridge England, 2007; pp. 1-662.
6. <https://www.european-bioplastics.org/market/market-drivers/> (visited November 2018).
7. Park, D.H.; Hwang, S.J.; Oh, J.M.; Yang, J.H.; Choy, J.H. Polymer–inorganic supramolecular nanohybrids for red, white, green, and blue applications. *Prog. Polymer. Sci.* **2013**, *38*, 1442-1486.
8. Rossi, C.; Schoubben, A.; Ricci, M.; Perioli, L.; Ambrogio, V.; Latterini, L.; Aloisi, G. G.; Rossi, A. Intercalation of the radical scavenger ferulic acid in hydrotalcite-like anionic clays. *Int. J. Pharm.* **2005**, *295*, 47–55.
9. Yamada, H.; Tamura, K.; Watanabe, Y.; Iyi, N.; Morimoto, K. Geomaterials: their application to environmental remediation. *Sci. Technol. Adv. Mater.* **2011**, *12*, 064705 (13pp).
10. Sisti, L.; Totaro, G.; Fiorini, M.; Celli, A.; Coelho, C.; Hennous, M.; Verney, V.; Leroux, F. Poly(butylene succinate)/layered double hydroxide bionanocomposites: Relationships between chemical structure of LDH anion, delamination strategy, and final properties. *J. Appl. Polym. Sci.* **2013**, *130*, 1931-1940,
11. Leroux, F.; Dalod, A.; Hennous, M.; Sisti, L.; Totaro, G.; Celli, A.; Coelho, C.; Verney, V. X-ray diffraction and rheology cross-study of polymer chain penetrating surfactant tethered layered double hydroxide resulting into intermixed structure with polypropylene, poly(butylene)succinate and poly(dimethyl)siloxane. *Appl. Clay Sci.* **2014**, *100*, 102–111.
12. Totaro, G.; Sisti, L.; Celli, A.; Askanian, H.; Verney, V.; Leroux, F. Poly(butylene succinate) bionanocomposites: a novel bio-organo-modified layered double hydroxide for superior mechanical properties. *RSC Adv.* **2016**, *6*, 4780–4791.
13. Totaro, G.; Sisti, L.; Celli, A.; Hennous, M.; Askanian, H.; Verney, V.; Leroux, F. Chain extender effect of 3-(4-hydroxyphenyl)propionic acid/layered double hydroxide in PBS bionanocomposites. *Europ. Polym. J.* **2017**, *94*, 20–32.
14. Leroux, F.; Verney, V.; Sisti, L.; Celli, A.; Totaro, G. WO2016189228 A1, PCT/FR2016/051189, 12/01/2016.
15. Totaro, G.; Sisti, L.; Celli, A.; Aloisio, I.; Di Gioia, D.; Marek, A.; Verney, V.; Leroux, F. Dual chain extension effect and antibacterial properties of biomolecules interleaved within LDH dispersed into PBS by in situ polymerization. *Dalton Trans.* **2018**, *47*, 3155-3165.
16. Marek, A.A.; Verney, V.; Totaro, G.; Sisti, L.; Celli, A.; Leroux, F. Composites for « white and green » solutions: Coupling UV resistance and chain extension effect from poly(butylene succinate) and layered double hydroxides composites. *J. Solid State Chem.* **2018**, *268*, 9–15.
17. Sisti, L.; Totaro, G.; Celli, A.; Diouf-Lewis, A.; Verney, V.; Leroux, F. A new valorization route for Olive Mill wastewater: Improvement of durability of PP and PBS composites through multifunctional hybrid systems. *J. Environ. Chem. Eng.* **2019**, *7*, 103026.
18. Goula, A.M.; Lazarides, H.N. Integrated processes can turn industrial food waste into valuable food by-products and/or ingredients: The cases of olive mill and pomegranate wastes. *J. Food Eng.* **2015**, *167*, 45–50.
19. Totaro, G.; Sisti, L.; Vannini, M.; Marchese, P.; Tassoni, A.; Lenucci, M.S.; Lamborghini, M.; Kalia, S.; Celli, A. A new route of valorization of rice endosperm by-product: production of polymeric biocomposites. *Composites Part B* **2018**, *139*, 195–202.
20. Jiang L.; Zhang, J. Biodegradable and biobased polymers in Applied Plastics Engineering Handbook: Processing and Materials by Myer Kutz, 2011, William Andrew Ed. Elsevier, Oxford UK.
21. Coelho, C.; Hennous, M.; Verney, V.; Leroux, F. Functionalisation of polybutylene succinate nanocomposites: from structure to reinforcement of UV-absorbing and mechanical properties. *RSC Adv.* **2012**, *2*, 5430-5438.
22. Yoo E.S.; Im S.S. Melting Behavior of Poly(butylene succinate) during Heating Scan by DSC. *J. Polym. Sci. B: Polym. Phys.* **1999**, *37*, 1357–1366.
23. Pavlidou, S.; Papaspyrides, C.D. A review on polymer–layered silicate nanocomposites. *Prog. Polym. Sci.* **2008**, *33*, 1119–1198.
24. Sisti, L.; Cruciani, L.; Totaro, G.; Vannini, M.; Berti, C.; Tobaldi, D.M.; Tucci, A.; Di Gioia, D.; Aloisio, I.; Commereuc, S. TiO₂ deposition on the surface of activated fluoropolymer substrate. *Thin Solid Films* **2012**, *520*, 2824–2828.

25. Sisti, L.; Cruciani, L.; Totaro, G.; Vannini, M.; Berti, C.; Aloisio, I.; Di Gioia, D. Antibacterial coatings on poly(fluoroethylenepropylene) films via grafting of 3-hexadecyl-1-vinyl imidazolium bromide. *Prog. Org. Coat.* **2012**, *73*, 257-263.
26. Carraro, L.; Fasolato, L.; Montemurro, F.; Martino, M.E.; Balzan, S.; Servili, M.; Novelli, E.; Cardazzo, B. Polyphenols from olive mill waste affect biofilm formation and motility in *Escherichia coli* K-12. *Microb. biotechnol.* **2014**, *7*(3), 265-275.
27. Yakhlef, W.; Arhab, R.; Romero, C.; Brenes, M.; de Castro, A.; Medina, E. Phenolic composition and antimicrobial activity of Algerian olive products and by-products. *LWT.* **2018**, *93*, 323-328.
28. Leouifoudi, I.; Harnafi, H.; Ziyad, A. Olive mill waste extracts: polyphenols content, antioxidant, and antimicrobial activities. *Adv. Pharmacol. Sci.* **2015**, *2015*, 714138 (1-11pages).
29. Maris, P. Modes of action of disinfectants. *Rev. sci. tech. Off. int. Epiz.* **1995**, *14*(1), 47-55.
30. Totaro, G.; Marchese, P.; Sisti, L.; Celli, A. Use of ionic liquids based on phosphonium salts for preparing biocomposites by *in situ* polymerization. *J Appl Polym Sci* **2015**, *132*, 42467-42475.
31. Lala, N.L.; Ramaseshan, R.; Bojun, L.; Sundarajan, S.; Barhate, R.S.; Ying-jun, L.; Ramakrishna, S.; (). Fabrication of nanofibers with antimicrobial functionality used as filters: protection against bacterial contaminants. *Biotechnology and Bioengineering* **2007**, *97*(6), 1357-1365.
32. Barahuie, F.; Hussein, M.Z.; Gani, S.A.; Fakurazi S.; Zaina, Z. Synthesis of protocatechuic acid-zinc/aluminium-layered double hydroxide nanocomposite as an anticancer nanodelivery system. *J. Solid State Chem.* **2015**, *221*, 21-31].
33. Kim, H.J.; Ryu, K.; Kang, J.H.; Choi, A.J.; Kim, T.I.; Oh, J.M. Anticancer Activity of Ferulic Acid-Inorganic Nanohybrids Synthesized via Two Different Hybridization Routes, Reconstruction and Exfoliation-Reassembly. *The scientific world journal* **2013**, *2013* art ID 421967 (9 pages).
34. Privas, E.; Leroux, F.; Navard, P. Preparation and properties of blends composed of lignosulfonated layered double hydroxide/plasticized starch and thermoplastics. *Carbohydr. Polym.* **2013**, *96*, 91-100.